KCI CONRETE JOURNAL
Vol.14 No.1, March 2002, pp.51-60

Static and Fatigue Behavior of RC Beams Strengthened with Steel Plates

Byung-Hwan Oh[1], Jae-Yeol Cho[2]*, and Soo-Won Cha[3]

[1] *Professor, Department of Civil Engineering, Seoul National University, Korea*
[2] *Special Researcher, Research Institute of Engineering Science, Seoul National University, Korea*
[3] *Department of Civil Engineering, Hankyong National University, Korea*

(Received December 6, 2001; Accepted January 28, 2002)

Abstract

Strengthening of existing concrete structures is a major concern in recent years as the number of degraded structures increases. The purpose of this paper is to investigate the static and fatigue behavior of reinforced concrete (RC) beams strengthened with steel plates. To this end, a comprehensive test program has been set up and many series of strengthened beams have been tested. The major test variables include the plate thickness, adhesive thickness, and the shear-span to depth ratio. The test results indicate that the separation of plates is the dominant failure mechanism even for the full-span-length strengthened beams with steel plate. The theoretical ultimate load capacities for strengthened beams based on the full composite action of concrete beam and steel plate are found to be larger than the actual measured load capacities. The strengthened beams exhibit more dominant shear cracking as the shear-span to depth ratio decreases. The ultimate capacity of strengthened beams increases slightly with the increase of adhesive thickness, which may be caused by the late initiation of plate separation in the beams with thicker adhesive. A realistic concept of ductility for plate-strengthened beams is proposed in this study. It is seen that the strengthened beams show relatively low ductility compared with unstrengthened beams. The present study indicates that the strengthened beams exhibit much higher fatigue resistance than the unstrengthened beams. The increase of deflections of strengthened beams according to the number of load cycles is much smaller than that of unstrengthened beams. The present study provides very useful results for the realistic application of plate-strengthening method in reinforced concrete structures.

Keywords: strengthening, concrete structure, fatigue, steel plate, separation

1. Introduction

In recent years, with the development of structurally effective adhesives, the plating methods have been widely used for strengthening of existing concrete structures.[2,4,5,9-11,15,16] The plate-bonding method often has, however, a serious premature failure problem due to the separation of plates and rip-off of concrete along the tensile reinforcing bars. In this regard, many studies have been conducted to investigate the failure behavior of strengthened beams with steel plates.[3,6,8,14,17] Swamy et al. carried out extensive tests on the beams strengthened with the steel plates and reported that the steel plating can increase the ultimate flexural strength by up to about 15%.[15,16] Jones et al. studied the effects of anchorage details on the failure behavior of strengthened beams with steel plates and reported that the anchorage details had some effects on the ultimate strength and failure modes.[6] However, they found that anchor bolting does not prevent the debonding of strengthened plates. Hussain et al. also reported that the premature failure of strengthened beams is closely related to the plate thickness and that the end anchorage cannot totally prevent the premature failure.[5] Hamoush and Ahmad published similar research results on the debonding of steel-strengthened concrete beams through the tests of five plain concrete beams.[3] The authors also studied on the failure behavior of strengthened beams with steel plates and presented useful experimental data.[11] Although there exist some good static test data from eminent researchers mentioned previously, these are not enough to fully capture the failure and the ductility behavior of beams strengthened with steel plates.

* *Corresponding author*
Tel.: +82-2-880-8310; Fax.: +82-2-880-0349
E-mail address: cjyshk@hananet.net

On the other hand, even though there are some test data on the structural behavior of strengthened beams under monotonic static loading, it is very difficult to find the existing test data on the fatigue behavior of strengthened beams with steel plates under repetitive loadings.

The purpose of the present paper is, therefore, to explore the static and fatigue behavior of concrete beams externally strengthened and reinforced with steel plates under monotonic and repeated loadings.

2. Static and fatigue tests of strengthened beams

2.1 Design of test beams

An extensive experimental program was set up to investigate the structural behavior of flexure-strengthened reinforced concrete beams with steel plates. A total of 20 reinforced concrete beams (i.e., 19 strengthened beams and one unstrengthened control beam) have been tested. The dimension of test beams is 150mm × 250mm × 2400mm as shown in Fig. 1. Among them, 14 beams were tested under static load and the other six beams were tested under repetitive fatigue loads. Each beam has two tensile reinforcing bars of D16 and two compressive steel bars of D13. The stirrups were symmetrically placed as shown in Fig. 1 with the spacing of 110mm. The spacing of stirrups, and maximum and minimum reinforcement ratios are in accordance with the provision of ACI 318-99 Code.

2.2 Major test variables

The main test variables considered in the present study include the plate thickness, adhesive thickness, and shear-span to depth ratio. The plate thickness varies from 2 to 5 mm and the adhesive thickness varies from 1 to 7 mm. The shear-span to depth ratios are 1.36 ~ 4.77. Those test variables are summarized in Table 1. For all beams the length of the bonded plate is 2,000 mm, which covers almost the full span length between supports of the beams (see Fig. 2), and the plate width is 150 mm which is the same as beam width. The reason for the full-span length strengthening with steel plates is to maximize the strengthening effects by delaying the plate separation.

For the fatigue tests, the main test variable is the ratio of applied load to the failure load of the reference beam. The applied load levels are 60, 70, and 80 percent of the failure load of the reference beam (beam S43), respectively (Table 1). The reference beam S43 for the fatigue tests is selected such that it has the intermediate values for strengthening parameters.

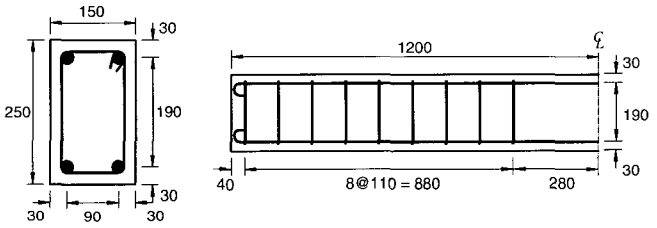

Fig. 1 Beam details of test specimen (unit: mm)

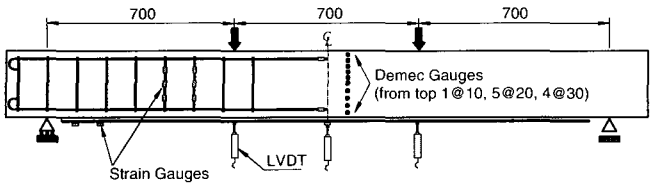

Fig. 2 Details of measurement schemes (unit: mm)

2.3 Material properties

The ordinary Portland cement (Type I) was used and the maximum size of coarse aggregate is 25mm. The mixture proportion is given in Table 2.

Table 1 Test parameters and specimen identifications

Beam ID	Test type	Plate thickness (mm)	Adhesive thickness (mm)	Shear-span to depth ratio(a/d)
Control	Static	-	-	3.18
S23	Static	2	3	3.18
S33	Static	3	3	3.18
S43	Static	4	3	3.18
S53	Static	5	3	3.18
S41	Static	4	1	3.18
S43	Static	4	3	3.18
S45	Static	4	5	3.18
S47	Static	4	7	3.18
S43S1	Static	4	3	4.77
S43S2	Static	4	3	4.09
S43	Static	4	3	3.18
S43S3	Static	4	3	2.27
S43S4	Static	4	3	1.36
Cont-F60	Fatigue	-	-	3.18
F60	Fatigue	4	3	3.18
F70	Fatigue	4	3	3.18
F80	Fatigue	4	3	3.18

Table 2 Mixture proportion of concrete

Slump (mm)	Air content (%)	W/C (%)	Contents (kg/m^3)			
			Water	Cement	Coarse agg.	Fine agg.
150	4.5	43.8	171	390	969	768

The compressive strengths of concrete were measured from three cylinders after 28 days curing according to ASTM C 39. The average compressive strength is 28.7 MPa (design strength 28.0 MPa). Two tensile reinforcing bars of D16 were used, yield strength of which measured is 365 MPa, and measured tensile strength is 536 MPa. The compressive reinforcing bars have a diameter of 13 mm with the measured yield strength of 345 MPa and tensile strength of 503 MPa (Fig. 1). The modulus of elasticity of steel bars is 200 GPa. The stirrups of D6 are symmetrically spaced as shown in Fig. 1. The measured yield strength of stirrup is 420 MPa and the tensile strength is 600 MPa and the modulus of elasticity is 200 GPa. For strengthening of beams, the rolled structural steel was used. The yield and tensile strengths of plates are 292 MPa and 410 MPa, respectively. Above all material properties were measured from actual laboratory tests. A low viscous epoxy was injected to achieve the predetermined adhesive thickness as shown in Table 1. The compressive strength, tensile strength and modulus of elasticity of epoxy materials are 180 MPa, 70 MPa and 2,300 MPa, respectively.

2.4 Plates bonding procedure

The concrete surface treatment prior to plating works is very important to guarantee the perfect bonding between two materials. Concrete was ground with a hand grinder to expose the coarse aggregates and dusts were blown out by air compressor. After the surface treatment, putty was applied to fill up the cavities or holes. The surface of steel plate was sand-blasted to eliminate the rust and membrane formed by heat treatment. The epoxy was injected into the gap between the concrete surface and steel plate, while maintaining the gap to achieve the required adhesive thickness. The epoxy-injected beams were cured for sufficiently long time.

2.5 Measurement and test scheme

Fig. 2 shows the locations of measuring sensors including strain gages and linear variable differential transformers (LVDT). The steel strain gages were attached on the surfaces of strengthened steel plate and internal reinforcing bars (Fig. 2). The demec gages are also attached along the height of beam at the midspan region to measure the horizontal strains. These values can be used to find the strain distribution and the neutral axis depth.

The static load is applied step-by-step up to 70kN in a load control manner and then shifted to displacement control method up to the failure of test beams. The combination of loading method is to perform the tests efficiently while obtaining full history of failure behavior. The rate of displacement is 0.05 mm/sec.

In fatigue test, the maximum levels of load are 60 % (76kN), 70 % (88kN), 80 % (100kN) of the static failure load (126kN) for reference beam S43, respectively. The minimum load level is set to 10kN. The frequency of fatigue load is 3 Hz and the repetition of load is continued up to 4,000,000 cycles, if not failed.

3. Test results and discussions on static tests

3.1 Failure modes

Fig. 3 shows the failure and cracking patterns for various test beams. The control beam without strengthening plates shows the traditional flexural failure because it was designed to fail in flexure. Fig. 3 indicates that the strengthened beams show shear-type failure with many diagonal cracks, which was caused by the increase of flexural capacities due to steel plates. Most of the test beams exhibited the separation of steel plates, even though the beams were strengthened for full span length between supports. The diagonal cracks occurred with the separation of steel plates.

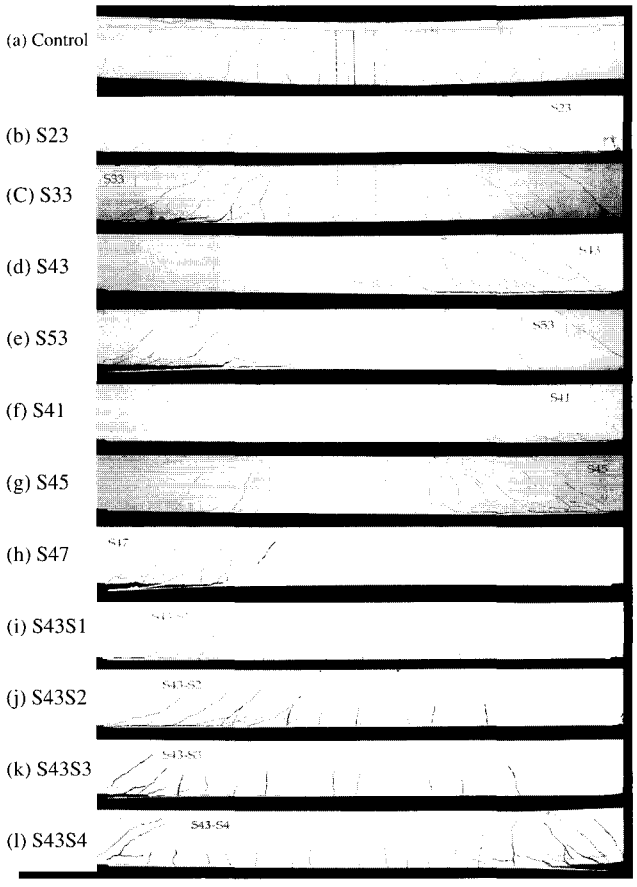

Fig. 3 Failure configuration of steel plated beams at ultimate state

Table 3 *Test results for steel plated beams*

Beam ID	Separation load P_{sep} (kN)	Peak load P_{ult} (kN)	Ratio to unstrengthened beam	at P_{ult}				Failure mode[3]
				Displacement (mm)	Strains (μ)			
					Steel plate ($1{,}400\mu$)[2]	Tensile rebar ($1{,}800\mu$)[2]	Stirrup ($2{,}100\mu$)[2]	
Control	-	89(79)[1]	1.00	34.7(7.2)[1]	-	>>1,800	691	Flexure
S23	131	136	1.53	8.15	>>1,400	1,633	1,825	PY,PS,DT
S33	129	137	1.54	7.02	1,288	1,484	1,222	PY,PS,DT
S43	126	126	1.42	4.35	1,079	1,040	581	PS,DT
S53	132	142	1.60	5.00	1,005	835	898	PS,DT
S41	120	125	1.40	4.68	1,090	1,220	1,022	PS,DT
S43	126	126	1.42	4.35	1,079	1,040	581	PS,DT
S45	134	134	1.51	4.97	1,172	1,045	879	PS,DT
S47	140	150	1.69	5.35	1,244	1,207	1,004	PS,DT
S43S1	129	132	1.48	5.94	1,913	1,642	594	PY,PS,DT
S43S2	127	128	1.44	5.61	1,427	1,266	593	PS,DT
S43	126	126	1.42	4.35	1,079	1,040	581	PS,DT
S43S3	131	135	1.51	4.67	869	793	447	PS,DT
S43S4	214	221	2.48	5.13	691	689	1015	SC,PS

Note: 1) The value in parenthesis ( ) represents the measurement at yielding of rebar, 2) Represent the yield strains given from actual material test, 3) PS=Plate Separation, PY=Plate Yielding, DT=Diagonal Tension Failure

Fig. 3 also indicates that the beams with thicker plates exhibit more shear cracking and larger separation. It is also seen that the shear-span to depth ratios (a/d) have great effect on the failure modes (see Fig. 3(h)~(l)). The beams with small a/d showed dominant shear failure with smaller flexural cracks (Fig. 3(l)). The effects of these parameters will be examined in more detail in the next section.

Table 3 summarizes the test results for the separation loads, peak loads, displacements and strains at the peak loads, and the failure modes for the tested beams. It can be seen that the peak load is not much larger than the separation load and almost the same as separation load for each beam. This means that the separation failure is the predominant failure mechanism in the beams strengthened with steel plates. Table 3 also shows the increase of peak load according to the various strengthening of plates. The rates of increase of peak loads range from 40 to 70% depending upon the strengthening method.

3.2 Calculation of flexural strength

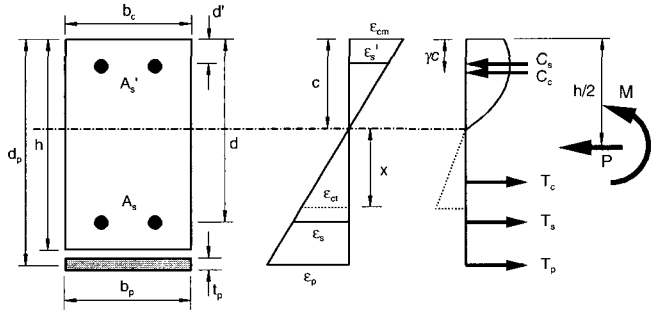

Fig. 4 Cross-section and stress and strain distributions

The flexural strengths for strengthened beams have been calculated based on the bending theory, but employing the full stress-strain relations for materials. This calculation also considers the tensile resistance of concrete. It is assumed here that the plane sections before bending remain plane after bending and that the stress-strain curves for concrete and steel are known. Fig. 4 shows the stress and strain distributions in the cross-section of strengthened reinforced concrete (RC) beam. Fig. 5 shows the stress - strain curves for concrete, reinforcing bars and steel plate, respectively. For a given compressive concrete strain ε_{cm} and an assumed depth of neutral axis C, the strains of tensile reinforcing bars, compressive reinforcing bars, and plate, respectively, ε_s , ε_s' ,and ε_p can be determined from the strain triangle of Fig. 4 as follows.

$$\varepsilon_s = \frac{d-c}{c}\varepsilon_{cm}\,, \quad \varepsilon_s' = \frac{c-d'}{c}\varepsilon_{cm}\,, \quad \varepsilon_p = \frac{d_p-c}{c}\varepsilon_{cm} \tag{1}$$

The stresses f_s , f_s' , and f_p corresponding to the strains ε_s , ε_s' , and ε_p can be obtained from the stress-strain curves of Fig. 5, and then the forces T_s , C_s , and T_p is obtained as

$$T_s = f_s A_s\,, \quad C_s = f_s' A_s'\,, \quad \text{and} \quad T_p = f_p A_p = f_p b_p t_p \tag{2}$$

For a given concrete strain ε_{cm} in the extreme compressive fiber, the compressive force C_c and its position can be obtained by introducing the parameters α and γ as follows.

$$C_c = \alpha f_{cm} b_c c \tag{3}$$

The mean stress factor α can be determined from the area under the curve as follows

$$\alpha = \frac{\int_0^{\varepsilon_{cm}} f_c d\varepsilon_c}{f_{cm}\varepsilon_{cm}} \tag{4}$$

The factor γ can be determined from the center of gravity using the first moment of area under the stress-strain curve.

$$\int_0^{\varepsilon_{cm}} f_c \varepsilon_c d\varepsilon_c = (1-\gamma)\varepsilon_{cm} \int_0^{\varepsilon_{cm}} f_c d\varepsilon_c \tag{5}$$

$$\gamma = 1 - \frac{\int_0^{\varepsilon_{cm}} f_c \varepsilon_c d\varepsilon_c}{\varepsilon_{cm} \int_0^{\varepsilon_{cm}} f_c d\varepsilon_c}$$

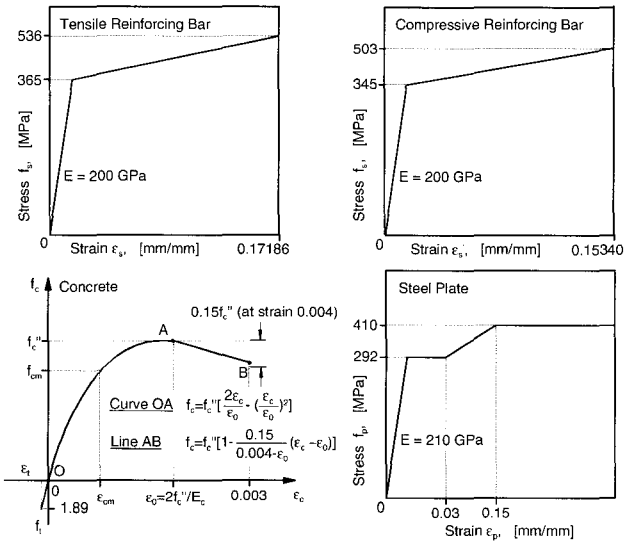

Fig. 5 Material models used in calculation

Table 4 Flexural strength of strengthened beams

Beam ID	Theoretical Flexural Strength		Measured Flexural Strength	$\frac{M_{n,t1}}{M_{n,m}}$	$\frac{M_{n,t2}}{M_{n,m}}$
	$M_{n,t1}$ (kN·m)	$M_{n,t2}$ (kN·m)	$M_{n,m}$ (kN·m)		
Control	28.4	30.8	31.2	0.91	0.99
S23	48.3	50.8	47.6	1.01	1.07
S33	57.1	60.6	48.0	1.19	1.26
S43	65.8	70.4	44.1	1.49	1.60
S53	73.9	80.2	49.7	1.49	1.61
S41	65.5	70.0	43.8	1.50	1.60
S43	65.8	70.4	44.1	1.49	1.60
S45	66.2	70.7	46.9	1.41	1.51
S47	66.5	71.1	52.5	1.27	1.35
S43S1	65.8	70.4	69.3	0.95	1.02
S43S2	65.8	70.4	57.6	1.14	1.22
S43	65.8	70.4	44.1	1.49	1.60
S43S3	65.8	70.4	33.8	1.95	2.08
S43S4	65.8	70.4	33.2	1.98	2.12

Similarly, the tension force T_c resisted by concrete can be considered as shown in Fig. 4. The distance x from the neutral axis to maximum tensile strain is obtained from Fig. 4 as Eq.(6). The tension force T_c and its acting position may be obtained from Eq.(7) and Eq.(8) respectively, where f_t is the tensile strength of concrete.

$$x = \frac{\varepsilon_t}{\varepsilon_{cm}} c = \frac{f_t}{E_c \varepsilon_{cm}} c \tag{6}$$

$$T_c = \frac{1}{2} f_t x b_c = \frac{1}{2} \frac{f_t^2 c b_c}{E_c \varepsilon_{cm}} \tag{7}$$

$$c + \frac{2}{3}x = \left(1 + \frac{2f_t}{3E_c\varepsilon_{cm}}\right)c \tag{8}$$

The force equilibrium equations can be written as

$$T_c + T_s + T_p - C_c - C_s = 0 \tag{9}$$

$$\frac{1}{2}\frac{f_t^2 c b_c}{E_c \varepsilon_{cm}} + f_s A_s + f_p b_p t_p - \alpha f_{cm} b_c c - f_s' A_s' = 0 \tag{10}$$

The resulting moment may now be derived as

$$M = \alpha f_{cm} b_c c\left(\frac{h}{2} - \gamma c\right) + f_s' A_s'\left(\frac{h}{2} - d'\right) + \frac{1}{2}\frac{f_t^2 c b_c}{E_c \varepsilon_{cm}}\left(c + \frac{2}{3}x - \frac{h}{2}\right) + f_s A_s\left(d - \frac{h}{2}\right) + f_p b_p t_p\left(d_p - \frac{h}{2}\right) \tag{11}$$

Table 4 shows the comparisons between the theoretical flexural strengths and the measured flexural strengths. The column (2) in Table 4 represents the theoretical flexural strength values calculated using the simple ACI Code equation and the column (3) represents the values obtained from the more accurate theory described in the previous section (Eqs.(1)~(11)). It is seen that the calculated values are overestimated greatly. This is due to the premature failure by plate separation in actual tests before achieving full strength.

3.3 Effect of steel plate thickness

As shown in Table 4, the theoretical flexural strengths, which are based on the full composite action of concrete beam and steel plate, increase with an increase of plate thickness. However, the measured flexural strengths do not show this tendency. This is because the strengthened beams failed by the premature separation of plate before reaching the yield point. Fig. 6 shows the effects of plate thickness on the load-deflection curves and load-rebar strains. Fig.

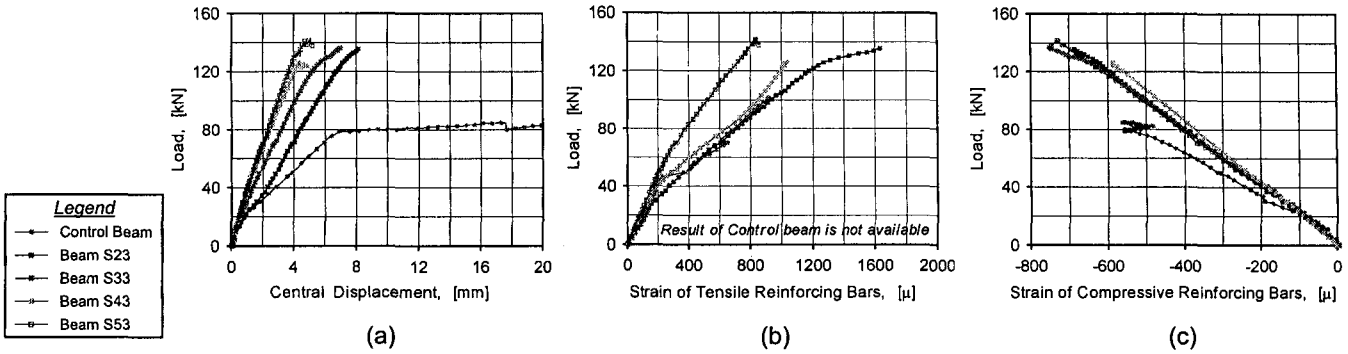

Fig. 6 Effect of plate thickness on the load-deflection curves and load-rebar strain relations

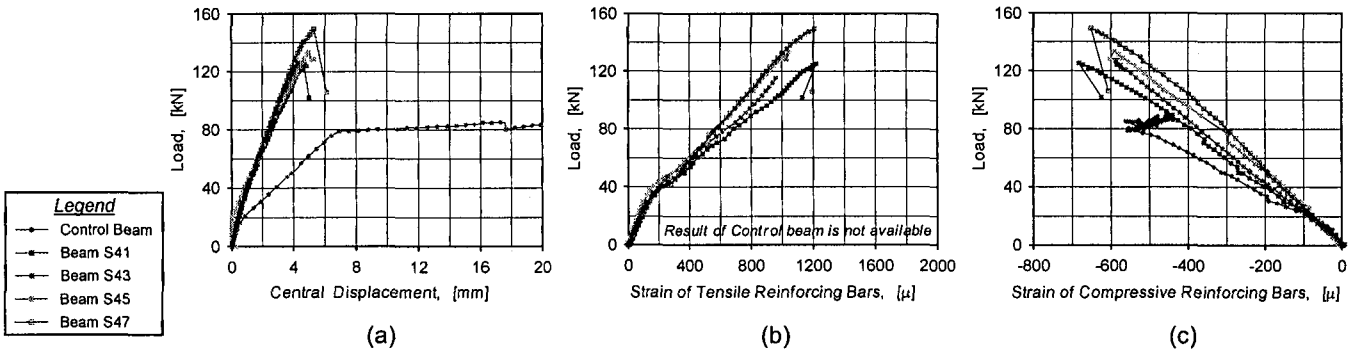

Fig. 7 Effect of adhesive thickness on the load-deflection curves and load-rebar strain relations

6(a) indicates that the central displacements of strengthened beams decrease as the thickness of plates increase. This effect can be also seen in the load-rebar strain relations (Fig. 6(b), (c)).

3.4 Effect of adhesive thickness

The effect of adhesive thickness on the flexural strength can be also seen in Table 4. The measured flexural strengths increase slightly with the increase of adhesive thickness, while the ideal theoretical ones do not change much according to the adhesive thickness. The increase of flexural strength with adhesive thickness may come from the late initiation of plate separation for the case of beam with thicker adhesive. Fig. 7 shows the effects of adhesive thickness on the load-deflection curves and load-rebar strains. It is seen that the strengthened beams exhibit much higher stiffness and peak loads than control beam, although the displacements at peak loads are rather small compared with those of unstrengthened control beams.

3.5 Effect of shear span to depth ratio

Fig. 8 shows the variation of ultimate load capacity according to the shear-span to depth ratio (a/d) for the beam series S43. Fig. 8 indicates that the measured load capacity does not vary much according to the shear-span to depth ration (a/d) except for the beam (S43S4) with very low a/d value (i.e., a/d = 1.36). However, the calculated load capacity increases with a decrease of a/d value, because the

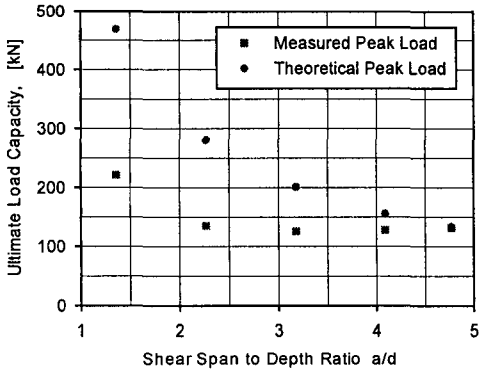

Fig. 8 Ultimate load capacities according to the shear span to depth ratio

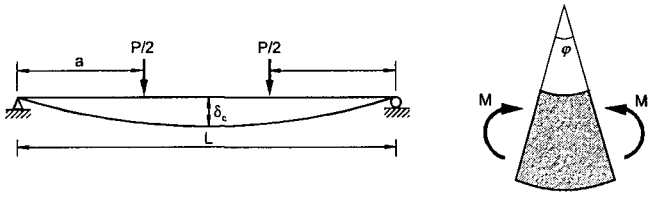

Fig. 9 Central displacement and moment curvature relation

beams were designed to fail in flexure and to posses higher shear capacity. This discrepancy is caused by the premature separation failure of strengthened plates. Therefore, the separation failure must be considered appropriately to assess realistically the ultimate capacities of strengthened beams with plates. The failure of strengthened beams due to plate separation can be predicted by introducing a concept of separation criterion, which was submitted separately by authors for publication.[12] This will not be addressed here due to the length of limitation of this paper and is beyond the scope of this paper.

3.6 Calculation of central displacements

The deflections at the midspan of the beams can be calculated by employing the relation between the displacement and the curvature. The midspan displacement for the two-point loading of Fig. 9 is expressed as,

$$\delta_c = \frac{Pa}{48EI}(3L^2 - 4a^2) \tag{12}$$

For $a = L/3$ in this study, Eq. (12) can be rewritten as

$$\delta_c = \frac{23PL^3}{1296EI} \tag{13}$$

By using the relation of curvature and moment, i.e., $\varphi = M/EI$, and by employing $M = PL/6$ for this load case, Eq. (13) can be rewritten as follows.

$$\delta_c = \frac{23L^2}{216}\frac{M}{EI} = \frac{23L^2}{216}\varphi \tag{14}$$

The curvature φ can be obtained from the procedure described in Eqs. (1)~(11) by using the following Eq. (15). This can be done step-by-step up to the maximum failure stage. Fig. 10 shows the comparison of calculated and measured load-displacement curves for the control unstrengthened beam and strengthened beam S23. It is seen that the comparisons was in fairly good agreement between calculated and measured values, even after peak load for control beam.

$$\varphi = \frac{\varepsilon_{cm}}{c} \tag{15}$$

3.7 Neutral axis depth and strain distributions along the height of beam

The longitudinal concrete strains along the height of beams were measured at midspan and plotted in Fig. 11. Fig. 11 and Table 5 indicate that the depths of neutral axis increase as the thickness of strengthening steel plate increases. This phenomenon can be easily expected from the principle of mechanics for stiffened beams.

3.8 Ductility

The ductility is one of the important factors in maintaining the safety of structures. The ductility of flexural members can be defined from the deflection

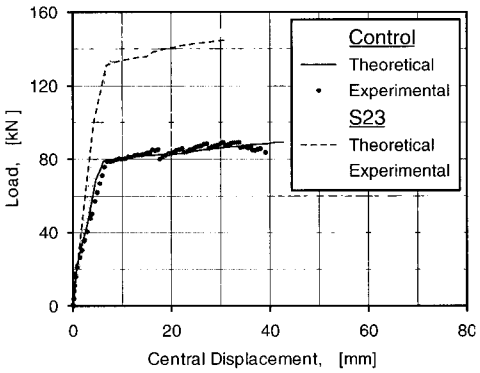

Fig. 10 Comparison of theoretical and experimental results on the central displacements

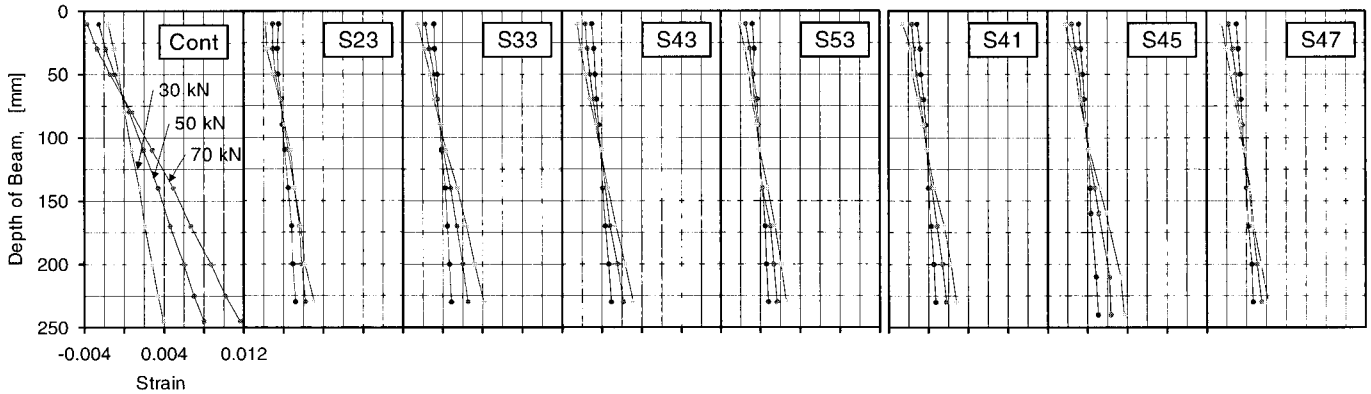

Fig. 11 Comparison of strain distributions and neutral axis depths for control and strengthened beams at each loading step

behavior as described in Eq. (16), where δ_y = the displacement at the yielding of tensile bars, δ_u = the displacement at the peak(maximum) load, and δ_p = the displacement at 75 percentile load after peak load, respectively (see Fig. 12).

$$\mu_{\delta 1} = \frac{\delta_u}{\delta_y}, \qquad \mu_{\delta 2} = \frac{\delta_p}{\delta_y} \tag{16}$$

The above deflection of ductility (Eq. (16)) may not be suitable for the strengthened beams because the failure of strengthened beam with steel plates is usually initiated by the premature separation of steel plates. Therefore, the ductility of strengthened beams with steel plates is proposed in this study as follows.

$$\mu_\delta = \frac{\delta_u}{\delta_s} \tag{17}$$

Where, δ_s = the displacement of strengthened beam at the initiation of plate separation or at the yielding of steel plate whichever comes first, and δ_u = the displacement at the maximum failure load (see Fig. 12). The value of ductility for control and strengthened beams are summarized in Table 5. Table 5 indicates that the strengthened beams exhibit very low ductility in contrast to unstrengthened ordinary beam, even though the ultimate load capacity increases greatly in strengthened beams.

Table 5 Depth of neutral axis (C) of strengthened beams at 70kN and ductility

Beam	Neutral Axis Depth			Ductility
	c, (mm)		*Test data* / *Theory*	μ_δ
	Theory	Test data		
Control	75	68	0.91	4.8
S23	98	92	0.94	1.1
S33	106	94	0.89	1.2
S43	113	113	1.00	1.0
S53	120	116	0.97	1.2
S41	113	112	0.99	1.1
S45	114	115	1.01	1.0
S47	114	120	1.05	1.1

Table 6 Summary of fatigue test results for unstrengthened beam and strengthened beams

Beam	P_{max} (kN)	No. of Cycles	P_{ult} (kN)	Failure modes
Cont-F60	53	1,352,455	-	Flexural failure
F60-1	76	4,000,000	120	Not fail
F60-2	76	-	-	Not available
F70-1	88	4,000,000	125	Not fail
F70-2	88	4,000,000	123	Not fail
F80-1	100	102,826	-	Plate separation
F80-2	100	83,245	-	Plate separation

4. Test results and discussions on fatigue tests

Fig. 13 explains how the fatigue loads have been applied to the beams. Measuring was planned to do approximately at every multiples of ten, but some additional measuring was intermittently done as the case may be. As shown in Fig. 13, after cyclic sine loading each measurement was carried out in the same pattern of static test with one cycle of loading and unloading. The fatigue tests were carried out for the strengthened beam series S43 as well as the unstrengthened control beam. The maximum load levels were 60, 70, and 80 % of the static failure load of the beam S43, respectively. Table 6 summarizes the results of fatigue tests. Table 6 indicates that the unstrengthened control beam failed in flexure at the load cycle of about 1.35×10^6 under 60 % fatigue load level, while the strengthened beams did not fail up to 4×10^6 cycles under the same 60 % fatigue load level. This means that the strengthened beam exhibits much higher fatigue resistance than the unstrengthened beam at the same fatigue load level. Table 6 also shows that the ultimate load capacities of the strengthened beams do not decrease even after load application of 4×10^6 cycles under 70 % fatigue load level. Under the 80 % fatigue load level, the strengthened beams failed at about 1×10^5 cycles by plate separation (Table 6).

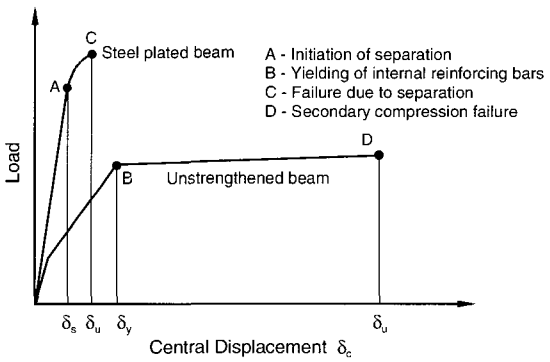

Fig. 12 Definition of ductility

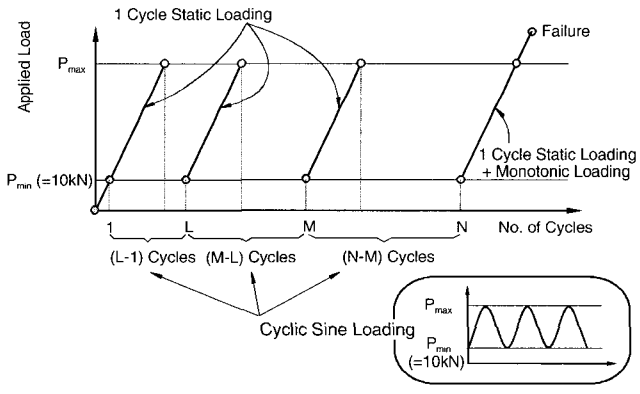

Fig. 13 Fatigue loading system

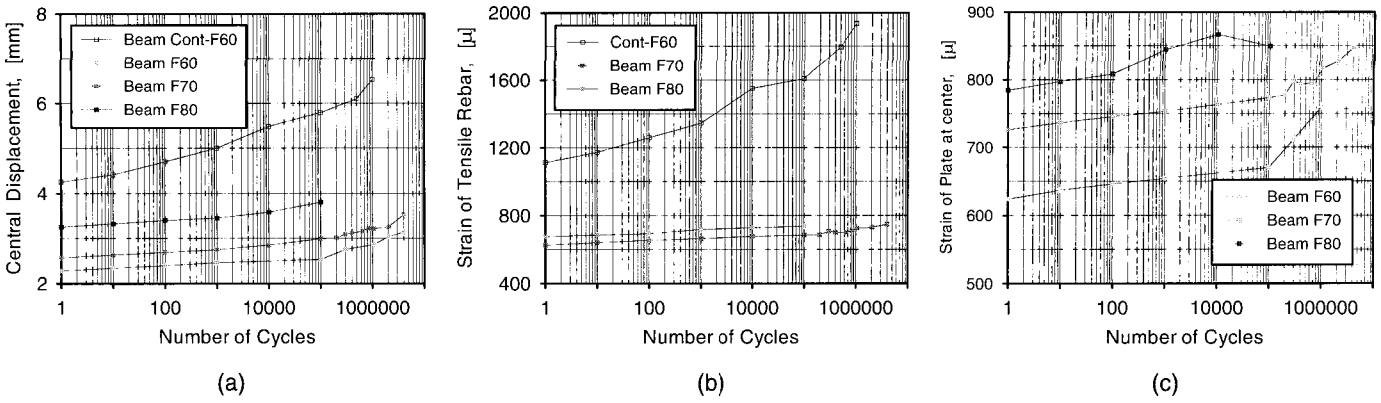

Fig. 14 Central displacement, tensile rebar strain, and strain of steel plate at center according to the number of fatigue-load cycles

Fig. 14 shows the variation of central deflections and tensile rebar strains according to the fatigue load cycles.

5. Conclusions

The purpose of the present study is to investigate the static and fatigue behavior of concrete beams externally strengthened with plates under monotonic and repeated loadings. The following conclusions have been drawn from the present study.

1) The flexure-strengthened beams with steel plates show shear-type failure with many diagonal cracks, while the unstrengthened control beams exhibit the conventional flexural failure.
2) The separation of plates is the predominant failure mechanism even for the full-span-length strengthened beams with steel plates. The ultimate loads are not much larger than the separation loads and almost the same as separation loads.
3) The theoretical ultimate load capacities for strengthened beams, which are based on the full composite action of concrete beam and steel plate, are found to the larger than the actual failure load capacities. This is due to the premature failure by the separation of plates in actual tests.
4) The ultimate capacities of strengthened beams increase slightly with the increase of adhesive thickness. This effect may be due to the late initiation of plate separation in the beams with thicker adhesive.
5) The strengthened beams show more dominant shear cracking with smaller flexural cracks as the shear-span to depth ratio decreases.
6) The calculated deflections based on the curvature and strain compatibility of the beam correlate very well with the test data.
7) A reasonable concept for the ductility of plate-strengthened beams is proposed. It is seen that the strengthened beams exhibit relatively low ductility compared with unstrengthened beams.
8) The present study indicates that the strengthened beams exhibit much higher fatigue resistance than the unstrengthened beams at the same fatigue load level.
9) The increase of deflections and strains of strengthened beams under fatigue loads is much smaller than that of unstrengthened beams.

The failure loads of strengthened beams due to plate separation can be predicted by introducing a separation criterion, which will be reported in a separate subsequent paper by authors.

ACKNOWLEDGEMENT

The experimental work presented in this paper was sponsored by Hyundai engineering & construction Co. Ltd. Financial support is greatly appreciated.

REFERENCES

1. American Concrete Institute (ACI), "*Building code requirements for structural concrete and commentary*," ACI 318-99, Farmington Hills, Mich, 1995.
2. Cho, J. Y., "*Behavior and analysis of RC beams strengthened with externally bonded plates for flexure and shear*," Ph.D thesis, Seoul National University, Seoul, Korea., 2001.
3. Hamoush, S. A. and Ahmad, S. H. (1990a), "Debonding of steel-strengthened concrete beams." *Journal of Structural Engineering, ASCE*, 116(2), 356-371.
4. Hamoush, S. A. and Ahmad, S. H. (1990b), "Static strength tests of steel strengthened concrete beams," *Materials and Structures*, France, 23, 116-125.
5. Hussain, M., Sharif, A., Basunbul, I. A., and Baluch, M. H., "Flexural behavior of precracked reinforced concrete beams strengthened externally by steel plates." *ACI Structural Journal*, 92(1), 1995, pp. 14-22.

6. Jones, R., Swamy, R. N., and Charif, A., "*Plate separation and anchorage of reinforced concrete beams strengthened by epoxy-bonded steel plates*," The Structural Engineer, London, 66(5), 1998, 85-94.
7. Mukhopadhyaya, P., Swamy, N., and Lynsdale, C., "Optimizing structural response of beams strengthened with GFRP plates," *Journal of Composites for Construction, ASCE*, 2(2), 1998, pp. 87-95.
8. Oehlers, D. J. and Moran, J. P., "Premature failure of externally plated reinforced concrete beams," *Journal of Structural Engineering, ASCE*, 116(4), 1990, pp. 978-993.
9. Oehlers, D. J. (1992), "Reinforced concrete beams with plates glued to their soffits," *Journal of Structural Engineering, ASCE*, 118(8), 1992, pp. 2023-2038.
10. Oehlers, D. J., Ali, M. S. M., and Luo, W., "Upgrading continuous reinforced concrete beams by gluing steel plate to their tension faces," *Journal of Structural Engineering, ASCE*, 124(3), 1998, pp. 224-232.
11. Oh, B. H., Cho, J. Y., and Kang, D. O., "Structural behavior of RC beams strengthened with steel," *Journal of Korea Concrete Institute*, Seoul (in Korean), 9(5), 1997, pp. 233-244.
12. Oh, B. H., Cho, J. Y., and Cha, S. W., "Failure behavior and separation criterion for strengthened concrete members with steel plates," *Journal of Korea Concrete Institute*, Seoul (in Korean), To be published, 2002.
13. Park, R., and Paulay, T. (1975), "Reinforced concrete structures." John Wiley & Sons.
14. Roberts, T. M. and Haji, K. H., "*Theoretical study of the behaviour of reinforced concrete beams strengthened by externally bonded steel plates*," Proc. Instn Civil Engrs Structs & Bldgs, 87, 1989, pp. 39-55.
15. Swamy, R. N., Jones, R., and Bloxham, J. W., "*Structural behaviour of reinforced concrete beams strengthened by epoxy-bonded steel plates*," The Structural Engineer, 65A(2), 1978, pp. 59-68.
16. Swamy, R. N., Jones, R., and Charif, A., "*The effect of external plate reinforcement on the strengthening of structurally damaged RC beams*," The Structural Engineer, London, 67(3), 1989, pp. 45-54.
17. Zhang, S. and Wood, L. A., "*Prediction of peeling failure of reinforced concrete beams with externally bonded steel plates*," Proc. Instn Civil Engrs Structs & Bldgs, 110, 1995, pp. 257-268.